



Contents lists available at ScienceDirect

Bioorganic & Medicinal Chemistry Letters

journal homepage: www.elsevier.com/locate/bmcl

Identification and optimisation of a series of tetrahydrobenzotriazoles as metabotropic glutamate receptor 5-selective positive allosteric modulators that improve performance in a preclinical model of cognition

John M. Ellard^a, Andrew Madin^a, Oliver Philps^a, Mark Hopkin^a, Scott Henderson^a, Louise Birch^a, Desmond O'Connor^c, Tohru Arai^d, Kazuma Takase^e, Louise Morgan^b, David Reynolds^b, Sonia Talma^b, Eimear Howley^b, Ben Powney^b, Andrew H. Payne^a, Adrian Hall^a, Jane E. Gartlon^b, Lee A. Dawson^b, Luis Castro^a, Peter J. Atkinson^{b,*}

^a Medicinal Chemistry, Neuroscience Product Creation Unit, Eisai Limited, European Knowledge Centre, Mosquito Way, Hatfield, Hertfordshire AL10 9SN, UK

^b Pharmacology, Neuroscience Product Creation Unit, Eisai Limited, European Knowledge Centre, Mosquito Way, Hatfield, Hertfordshire AL10 9SN, UK

^c DMPK, Neuroscience Product Creation Unit, Eisai Limited, European Knowledge Centre, Mosquito Way, Hatfield, Hertfordshire AL10 9SN, UK

^d Next Generation Systems Core Function Unit, Eisai Product Creation Systems, Eisai Co., Ltd, 5-1-3 Tokodai, Tsukuba, Ibaraki 300-2635 Japan

^e Biomarker and Personalized Medicine Core Function Unit, Eisai Product Creation Systems, Eisai Co., Ltd, 5-1-3 Tokodai, Tsukuba, Ibaraki 300-2635 Japan

ARTICLE INFO

Article history:

Received 27 August 2015

Revised 14 October 2015

Accepted 16 October 2015

Available online xxxxx

Keywords:

Metabotropic glutamate receptor 5 (mGlu5)

Positive allosteric modulator (PAM)

Cognition

Tetrahydrobenzotriazole

ABSTRACT

Herein we describe a series of tetrahydrobenzotriazoles as novel, potent metabotropic glutamate receptor subtype 5 (mGlu5) positive allosteric modulators (PAMs). Exploration of the SAR surrounding the tetrahydrobenzotriazole core ultimately led to the identification of **29** as a potent mGlu5 PAM with a low maximal glutamate potency fold shift, acceptable in vitro DMPK parameters and in vivo PK profile and efficacy in the rat novel object recognition (NOR) assay. As a result **29** was identified as a suitable compound for progression to in vivo safety evaluation.

© 2015 Published by Elsevier Ltd.

Glutamate is the major excitatory neurotransmitter in the central nervous system (CNS) and activates both ionotropic (α -amino-3-hydroxy-5-methyl-4-isoxazole propionic acid (AMPA), *N*-methyl-D-aspartate (NMDA) and kainate) and eight metabotropic glutamate receptors (mGlu1 to mGlu8). mGlu5 receptors are located extensively throughout the CNS and are physically and functionally associated with NMDA receptors, contributing to numerous synaptic events that underpin cognitive function.^{1–5}

The emergence of small molecule mGlu positive allosteric modulators (PAMs) has provided new opportunities for improved receptor subtype selectivity, tractability and regulatory control over traditional orthosteric agonists. These compounds typically enhance endogenous orthosteric ligand activation of the receptor (without producing any intrinsic activity alone), and are thus thought to limit potentially detrimental effects associated with conventional receptor agonists. Several distinct mGlu5 selective PAM chemotypes have been reported³ and numerous studies with

tool compounds support a pro-cognitive role for mGlu5. In vitro mGlu5 PAMs have been shown to enhance NMDA mediated synaptic plasticity and potentiate hippocampal LTP and LTD.⁴ These data are further supported by in vivo studies in which mGlu5 PAMs have been shown to increase performance in NOR, enhance hippocampal spatial learning in the Morris water maze and improve performance in the Y-maze spatial alternation task.^{4,5}

Despite promising advances in the development of novel CNS penetrant mGlu5 receptor PAMs, recent reports have emerged describing the occurrence of adverse events in pre-clinical in vivo studies. Conn et al. reported a lead example from a series of dihydroimidazopyrimidinones which exhibited CNS mediated adverse effects including pro-convulsive behaviour and dizziness.⁶ Researchers from Merck and Addex have also reported neurotoxicity with significant neuronal death observed, particularly in the auditory cortex, with three distinct mGlu5 PAMs following repeated dosing.⁷ In these studies it was suggested that compounds with relatively low in vitro efficacy exhibited an improved in vivo efficacy-toxicity window. In vitro PAM efficacy

* Corresponding author.

E-mail address: Peter_Atkinson@eisai.net (P.J. Atkinson).

is often determined by measuring the leftward shift (increase in potency) of the orthosteric ligand concentration–response curve (often referred to as ‘fold-shift’) in the presence of increasing concentrations of PAM compound. Thus, a PAM compound that exhibits a low maximal fold shift only produces a limited enhancement of signal at any given concentration of orthosteric ligand (in this case glutamate). Accordingly, Parmentier-Batteur et al. suggested that the unbound plasma concentration required for efficacy in an amphetamine-induced locomotor activity assay corresponded to an estimated 2 fold glutamate potency shift in vitro.⁷ It was therefore of interest to us to identify novel mGlu5 PAMs exhibiting low glutamate co-operativity (or ‘fold shift’) and investigate this link further.

Our efforts to discover novel mGlu5 PAM chemotypes consisted of three parallel approaches: A knowledge based design strategy, a focused HTS and a ligand based in silico screening approach which considered both the 3-dimensional shape and electronic features identified from known mGlu5 PAMs and was conducted using Cressett Fieldscreen. Each of these strategies provided novel mGlu5 PAM series which warranted further investigation. The benzotriazole (**1**, Fig. 1) was identified from in silico screening as a novel mGlu5 PAM chemotype with moderate potency and maximal efficacy (pEC₅₀ 6.4, 51% max).

Benzotriazole **1** also exhibited a higher than desirable cLogP (cLogP 4.2⁸) and a high degree of planarity and aromaticity. It was postulated that replacement of the benzotriazole core with an alternative 5,6-bicyclic system would provide a scaffold with reduced lipophilicity and with the potential to introduce an sp³ centre linking to the oxadiazole substituent. This led to the identification of a tetrahydrobenzotriazole scaffold exemplified by **9** (Table 1) with a 10 fold improvement in potency and higher efficacy than the benzotriazole hit (**1**).

Initially these systems were prepared with the ‘reversed’ isomeric oxadiazole to that found in the benzotriazole hit **1** since these analogues were more readily accessible in a reduced number of synthetic steps (Scheme 1). The benzotriazole intermediates **5** were readily prepared in three steps by nucleophilic substitution between an appropriate amine and methyl 4-fluoro-3-nitrobenzoate, followed by reduction of the nitro group, diazotisation and subsequent cyclisation.⁹ Reduction of the aromatic ring was accomplished by hydrogenation at 100 °C and 100 bar of hydrogen gas over palladium on carbon to provide the tetrahydrobenzotriazole (**6**). Following hydrolysis of the methyl ester the 1,2,4-oxadiazole (**8**) was formed by EDC mediated coupling with an *N*-hydroxyamidine and then cyclisation in refluxing 1,4-dioxane. The individual enantiomers of the tetrahydrobenzotriazoles were separated by preparative chiral HPLC.

Resolution via diastereomeric salt formation with (1*S*,2*S*)-2-amino-1-(4-nitrophenyl)propane-1,3-diol and the carboxylic acid intermediate **7** was also accomplished where R¹ was *tert*-butyl. The chiral intermediates obtained in this manner were progressed to provide single enantiomers of the fully substituted tetrahydrobenzotriazoles. A small molecule X-ray structure of the diastereomeric salt was used to confirm that the enantiomer of the carboxylic acid intermediate which gave rise to the most

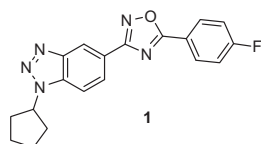


Figure 1. Initial benzotriazole hit.

Table 1
Triazole substituents

Example	R-group	pEC ₅₀ ^c (% max)	Maximal glutamate fold shift ^d
9^a		7.5 (103)	10
10^a		6.4 (78)	4 ^e
11^a		7.8 (106)	3 ^e
12^a		<4.6	n.t. ^f
13^b		5.4 (91)	n.t.
14^a		6.4 (96)	4
15^b		6.4 (98)	n.t.
16^a		8.3 (98)	4
17^a		8.0 (103)	7
18^a		7.5 (108)	8 ^e
19^a		7.8 (71)	3

^a Single enantiomer.

^b Racemic.

^c Ca²⁺ flux PAM assay (in the presence of EC₂₀ glutamate) utilising human U2OS cells expressing human recombinant mGlu5 receptors; % max, compound response (up to 25 μM) relative to the maximal glutamate response. Data represent mean of n ≥ 2.

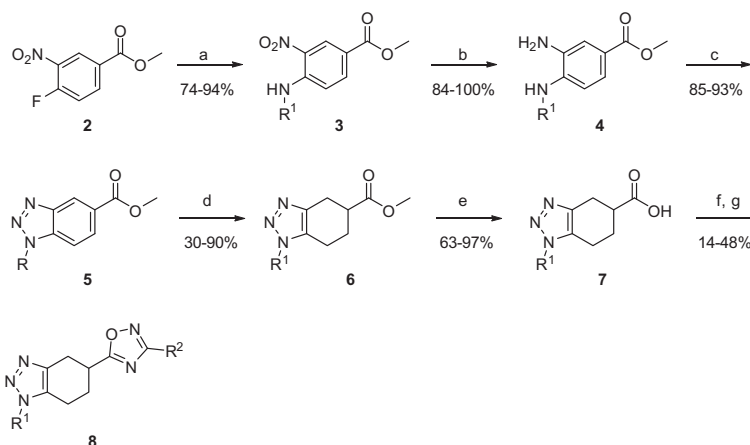
^d Maximal leftward shift in the EC₅₀ of glutamate induced by increasing concentrations (up to 25 μM) of test compound measured in rat cortical astrocytes. Unless otherwise stated n ≥ 3.

^e n < 3.

^f n.t. = not tested.

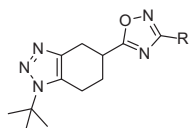
potent tetrahydrobenzotriazole enantiomers had (*S*) absolute stereochemistry.

As evidenced by the two enantiomers of the cyclopentyl analogue (**9** and **10**, Table 1) there was a clear enantiomeric preference for potency. Early exploration of the triazole substituent determined that non-aromatic groups had an optimal balance of properties. Despite having good potency, the 4-fluorophenyl analogue (**11**) imparted very low solubility and a high degree of brain tissue binding (Fu_{brain} 0.3%) while the 3-pyridyl analogue (**12**) was found to be inactive. Substituents bearing basic nitrogen atoms were also found to poorly tolerated, for example the piperidine derivative (**13**) displayed low activity. The cyclopentyl analogue (**9**) had good potency but suffered with a high glutamate fold shift and rapid microsomal clearance (rat Cl_{int} 146 μl/min/mg). While the microsomal stability (rat Cl_{int} 22 μl/min/mg) and glutamate fold shift was improved by the tetrahydrofuran substituent (**14**) this



Scheme 1. Reagents and conditions: (a) R^1NH_2 , DIPEA, NMP, rt, 16 h; (b) H_2 , 10% Pd/C, EtOAc, rt, 16 h; (c) $NaNO_2$, AcOH, H_2O , rt, 2 h; (d) H_2 , 10% Pd/C, AcOH, 100 °C, 100 bar, 2 x 16 h; (e) 1 M NaOH, MeOH, rt, 2 h; (f) $R^2C(OH)NH_2$, EDC, HOBt, DIPEA, DMF, rt, 16 h; (g) 1,4-dioxane, reflux, 4 h.

Table 2
Oxadiazole substituents



Example	R-group	pEC ₅₀ ^c (% max)	Maximal glutamate fold shift ^d
16 ^b		8.3 (98)	4
20 ^a		5.8 (67)	n.t. ^e
21 ^a		5.9 (29)	n.t. ^e
22 ^a		6.0 (66)	n.t.
23 ^a		6.7 (91)	n.t.
24 ^b		7.7 (77)	7 ^f
25 ^a		6.0 (68)	n.t.
26 ^b		7.1 (87)	6

^a Racemic.

^b Single enantiomer.

^c Ca^{2+} flux PAM assay (in the presence of EC₂₀ glutamate) utilising human U2OS cells expressing human recombinant mGlu5 receptors; % max, compound response (up to 25 μM) relative to the maximal glutamate response. Data represent mean of $n \geq 2$.

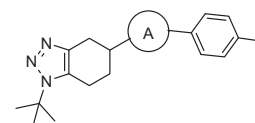
^d Maximal leftward shift in the EC₅₀ of glutamate induced by increasing concentrations (up to 25 μM) of test compound measured in rat cortical astrocytes. Unless otherwise stated $n \geq 3$.

^e n.t. = not tested.

^f $n < 3$.

analogue also had significantly lower mGlu5 PAM potency. The isopropyl substituent (**15**) provided moderate activity but the introduction of a tertiary substituent adjacent to the triazole ring was found to be optimal for potency with the *tert*-butyl analogue (**16**) displaying high potency and, importantly, a relatively low glutamate fold shift. The improvement in potency associated with a tertiary substituent is also evident with the methyltetrahydropry-

Table 3
Oxadiazole replacements



Example	Ring A	pEC ₅₀ ^c (% max)	Maximal glutamate fold shift ^d
16 ^a		8.3 (98)	4
27 ^a		8.3 (85)	5
28 ^b		5.5 (53)	n.t. ^e
29 ^a		7.3 (80)	3

^a Single enantiomer.

^b Racemic.

^c Ca^{2+} flux PAM assay (in the presence of EC₂₀ glutamate) utilising human U2OS cells expressing human recombinant mGlu5 receptors; % max, compound response (up to 25 μM) relative to the maximal glutamate response. Data represent mean of $n \geq 2$.

^d Maximal leftward shift in the EC₅₀ of glutamate induced by increasing concentrations (up to 25 μM) of test compound measured in rat cortical astrocytes. Unless otherwise stated $n \geq 3$.

^e not tested.

ran substituent (**17**), although this analogue suffered from a higher glutamate fold shift. The requirement for the tertiary centre to be proximal to the triazole ring is further supported by the drop in potency displayed by the *iso*-butyl analogue (**18**). The less lipophilic 2-methylpropanenitrile analogue (**19**) was also found to have good potency and one of the lowest glutamate fold shift observed in the series.

Substituted phenyl rings were found to be the optimal oxadiazole substituent (Table 2). The pyridyl analogue (**20**), displayed poor activity and saturated heterocycles such as morpholine **21** were only weakly active. Alkyl examples with the exception of the isobutyl analogue (**22**) were inactive and the cyclohexyl substituent (**23**) afforded only moderate potency. The benzyl analogue (**24**) also displayed good potency but suffered from very high microsomal clearance (rat Cl_{int} 120 $\mu l/min/mg$). While the *para*-fluoro phenyl (**16**) substituent did not impart an

Table 4
In vitro ADME profiles

Example	Human Cl_{int}^a ($\mu\text{l}/\text{min}/\text{mg}$)	Rat Cl_{int}^b ($\mu\text{l}/\text{min}/\text{mg}$)	MDCK P_{app} A to B ^c (10^{-6} cm^{-1})	MDCK efflux ratio ^d	Solubility ^e (μM)	Rat Fu_{brain}^f (%)
16	18	20	42	0.8	6	1.3
19	9	6	43	0.6	5.6	1.5
29	4	20	46	0.8	>100	5.6

^a 3 μM compound concentration, 0.5 mg/mL microsome concentration.^b 3 μM compound concentration, 0.5 mg/mL microsome concentration.^c Measured at 1 μM compound concentration.^d P_{app} A to B/ P_{app} B to A.^e Kinetic solubility 0.01 M phosphate buffered saline at pH7.4, 1% final DMSO concentration.^f Equilibrium dialysis from rat brain homogenate.**Table 5**
In vivo profiles

Example	Cl (ml/min/kg)	V_{ss} (L/kg)	$T_{max}/t_{1/2}$ (h) ^c	F^c (%)	C_{max} pl ^c (nM)	Total br:pl ^c	NOR MED ^d (mg/kg)
16	11 ^a	4.3 ^a	4.0/6.5	46	438	2.0	0.3
19	4 ^b	2.5 ^b	6.0/7.0	45	891	3.2	0.03 ^e
29	14 ^a	1.9 ^a	2.7/2.9	114	1946	1.4	0.3

^a Rat, i.v. 0.5 mg/kg.^b Rat i.v. 0.25 mg/kg.^c Rat p.o. 3 mg/kg.^d p.o. dosing with a 4 h pretreatment time ($n = 12$).^e Lowest efficacious dose (LED).

advantage in terms of potency (being equipotent to the *ortho*-fluoro, *meta*-fluoro or unsubstituted phenyl analogues), it is required for optimal microsomal stability. The fluoro substituent was identified as the preferred *para* substituent, being significantly more potent than other groups investigated such as dimethylamino **25** and nitrile **26**.

A number of replacements for the oxadiazole ring were also investigated (examples shown in Table 3). The 'reversed' oxadiazole **27** was found to exhibit comparable potency to **16** but with a marginally higher glutamate fold shift. In contrast, the 1,3,4-oxadiazole (**28**) suffered from a dramatic loss in potency. A promising alternative to the oxadiazole ring was found in the N-linked triazole analogue (**29**) which displayed a good balance of potency, ADME properties and a low glutamate fold shift.

As a result of the extensive SAR exploration, three compounds (**16**, **19** and **29**) from the series were identified which combined good mGlu5 PAM potencies, acceptable in vitro DMPK profiles and a relatively low maximal glutamate fold shift. Therefore these compounds were studied in greater detail.

The in vitro ADME profile of the compounds (Table 4) supported progression to in vivo studies. All three compounds possessed good apical to basal permeability in the MDCK-MDR1 permeability assay and were not subject to efflux. In contrast to **16** and **19** which had relatively low solubilities, **29** represented a significant improvement in solubility. This trend was also mirrored in the degree of brain tissue binding with **29** displaying an increased fraction unbound relative to **16** and **19**. In addition, these compounds did not exhibit significant inhibition of the Cyp isoforms tested. Moderate rat and human microsomal stability was observed for **16** while **29** exhibited moderate to low stability using rat and human liver microsomes respectively. In contrast, **19** could be considered a low clearance compound by both human and rat liver microsomes.

Each of **16**, **19** and **29** were found to be bioavailable and displayed good exposures following oral dosing to Sprague Dawley rats (3 mg/kg). Additionally they were found to display low plasma clearances, with moderate to high volumes of distribution. Both **16** and **19** also possessed long plasma half-lives and while **29** exhibited a slightly shorter half-life it was still acceptable for progression to behavioural studies (Table 5).

In considering reports of potential CNS safety liabilities associated with mGlu5 PAMs, compounds exhibiting good dose proportionality (relative to brain exposure) were favoured, thus enabling a clear safety margin to be determined in subsequent studies. In this regard, it was found that **29** exhibited good dose proportionality in rat up to at least 30 mg/kg p.o. The superior dose proportionality of **29** over **16** and **19** could be attributed at least in part to the far greater solubility of this analogue.

Following in vivo pharmacokinetic (PK) evaluation (Table 5) these compounds were evaluated in the rat NOR assay.¹⁰ All three compounds displayed a significant improvement in cognitive performance following a 4 hour pre-treatment time (minimal efficacious dose (MED) for **16** and **29** was 0.3 mg/kg, p.o. and for **19** the lowest efficacious dose (LED) was 0.03 mg/kg, p.o.). It was noted that, at the MED, the predicted unbound concentration of compound in the brain was lower than the functional EC₅₀ determined in vitro. We attribute this disparity partially to the sensitivity of the behavioural (NOR) model that was used (relative to other models). It is also possible that the in vitro functional calcium assay, while providing relative potency measurements for structure-activity and pharmacokinetic-pharmacodynamic purposes, may not fully recapitulate native receptor activity in the more complex in vivo system.

All three compounds were selective for the mGlu5 subtype with no detectable agonist, PAM or NAM activity at any of the other mGlu receptor subtypes (as determined by Euroscreen using a conventional concentration-response assay). A favourable selectivity profile was also observed when extending testing to a 55 member (ExpressProfile, Cerep) panel of receptors, ion channels and transporters.¹¹ In a hERG IonWorks assay **29** demonstrated weak inhibition (pIC₅₀ 5.2) however this was deemed tolerable when considering the relative plasma exposure at efficacious doses.

Based on these data **29** was identified as a potent mGlu5 PAM with good in vitro potency and a low maximal glutamate potency shift ratio. Further studies showed that Compound **29** demonstrated a favourable in vitro ADME and in vivo PK profile coupled with pro-cognitive efficacy in the NOR model in rats. This compound was therefore selected for progression into in vivo safety studies, results of which will be presented in a separate communication.

Acknowledgements

The authors would like to thank Dr. Dae-Shik Kim for the resolution of the acid **7**. The authors would also like to thank Dr. Andy Takle, Dr. Tomoyuki Shibuguchi, Dr. Yukio Ishikawa, Dr. Anne Cooper and Dr. Teiji Kimura for helpful discussions during the period of this work.

Supplementary data

Supplementary data (descriptions of the synthesis of **19** and **27** to **29**) associated with this article can be found, in the online version, at <http://dx.doi.org/10.1016/j.bmcl.2015.10.050>.

References and notes

- Ehlers, M. D. *Curr. Biol.* **1999**, *9*, R848.
- Alagarsamy, S.; Marino, M. J.; Rouse, S. T.; Gereau, R. W. T.; Heinemann, S. F.; Conn, P. J. *Nat. Neurosci.* **1999**, *2*, 234.
- Lindsley, C. W.; Stauffer, S. R. *Pharm. Pat. Anal.* **2013**, *2*, 93.
- (a) Conn, P. J.; Lindsley, C. W.; Jones, C. K. *Trends Pharmacol. Sci.* **2009**, *30*, 25; (b) Ayala, J. E.; Chen, Y.; Banko, J. L.; Sheffler, D. J.; Williams, R.; Telk, A. N.; Watson, N. L.; Xiang, Z.; Zhang, Y.; Jones, P. J.; Lindsley, C. W.; Olive, M. F.; Conn, P. J. *Neuropsychopharmacology* **2009**, *34*, 2057.
- (a) Balschun, D.; Zuschratter, W.; Wetzel, W. *Neuroscience* **2006**, *142*, 691; (b) Liu, F.; Grauer, S.; Kelley, C.; Navarra, R.; Graf, R.; Zhang, G.; Atkinson, P. J.; Popiolek, M.; Wantuch, C.; Khawaja, X.; Smith, D.; Olsen, M.; Kouranova, E.; Lai, M.; Pruthi, F.; Pulicicchio, C.; Day, M.; Gilbert, A.; Pausch, M. H.; Brandon, N. J.; Beyer, C. E.; Comery, T. A.; Logue, S.; Rosenzweig-Lipson, S.; Marquis, K. L. *J. Pharmacol. Exp. Ther.* **2008**, *327*, 827; (c) Uslander, J. M.; Parmentier-Batteur, S.; Flick, R. B.; Surles, N. O.; Lam, J. S.; McNaughton, C. H.; Jacobson, M. A.; Hutson, P. H. *Neuropharmacology* **2009**, *2009*, 531; (d) Reichel, C. M.; Schwendt, M.; McGinty, J. F.; Olive, M. F.; See, R. E. *Neuropsychopharmacology* **2010**, *36*, 782.
- Martín-Martín, M. L.; Bartolomé-Nebreda, J. M.; Conde-Ceide, S.; Alonso de Diego, S. A.; López, S.; Martínez-Vituro, C. M.; Tong, H. M.; Lavreysen, H.; Macdonald, G. J.; Steckler, T.; Mackie, C.; Bridges, T. M.; Daniels, J. S.; Niswender, C. M.; Noetzel, M. J.; Jones, C. K.; Conn, P. J.; Lindsley, C. W.; Stauffer, S. R. *Bioorg. Med. Chem. Lett.* **2015**, *25*, 1310.
- Parmentier-Batteur, S.; Hutson, P. H.; Menzel, K.; Uslander, J. M.; Mattson, B. A.; O'Brien, J. A.; Magliaro, B. C.; Forest, T.; Stump, C. A.; Tynebor, R. M.; Anthony, N. J.; Tucker, T. J.; Zhang, X. F.; Gomez, R.; Huszar, S. L.; Lamberg, N.; Fauré, H.; Le Poul, E.; Poli, S.; Rosahl, T. W.; Rocher, J. P.; Hargreaves, R.; Williams, T. M. *Neuropharmacology* **2014**, *82*, 161.
- Calculated using ChemDraw Ultra 12.0.
- Semple, G.; Skinner, P. J.; Cherrier, M. C.; Webb, P. J.; Sage, C. R.; Tamura, S. Y.; Chen, R.; Richman, J. G.; Connolly, D. T. *J. Med. Chem.* **2006**, *49*, 1227.
- Johnson, D. J.; Forbes, I. T.; Watson, S. P.; Garzya, V.; Stevenson, G. I.; Walker, G. R.; Mudhar, H. S.; Flynn, S. T.; Wyman, P. A.; Smith, P. W.; Murkitt, G. S.; Lucas, A. J.; Mookherjee, C. R.; Watson, J. M.; Gartlon, J. E.; Bradford, A. M.; Brown, F. *Bioorg. Med. Chem. Lett.* **2010**, *20*, 5434.
- <http://www.cerep.fr/cerep/users/pages/catalog/profiles/detailprofile.asp?profile=2117>.